AIAA JOURNAL
Vol. 41, No. 11, November 2003

Thin Airfoil in Fields of Nonuniform Density, Part 1: Single Density Interface

Frank E. Marble*
California Institute of Technology, Pasadena, California 91125

The classical theory of thin airfoils in unsteady low-speed flow, for example, von Kármán and Sears (von Kármán, T., and Sears, W. R., "Airfoil Theory for Non-Uniform Motion," *Journal of the Aeronautical Sciences*, Vol. 5, 1938, pp. 379–390) extended to the circumstance where the undisturbed flow contains certain regions of strong density variation. The unique feature of this situation is the vorticity generated in the regions of density gradient, which, in turn, induces additional loading on the airfoil in much the same manner as does the trailing vortex sheet in conventional unsteady airfoil theory. In a special case of this problem, Marble (Marble, F. E., "Response of a Thin Airfoil Encountering a Strong Density Discontinuity," *Symposium on Aerodynamics and Aeroacoustics*, edited by K.-Y. Fung, World Scientific, 1993; also *Journal of Fluids Engineering*, Vol. 115, 1993, pp. 580–589) introduced two concepts that substantially simplified an otherwise complicated situation. One was the application of Kelvin's theorem to flows where the fluid density had discontinuities that were transported with the fluid. The second and more essential simplication of the analysis was the development of a representation for the vorticity induced on a convected density interface in the form of "image" vortices of appropriate strength and location. The present analysis generalizes thin airfoil theory to include a single density interface convected past the airfoil at any angle with respect to the airfoil. For a single density interface, with the gas density upstream half that downstream, the results show strong variations in pressure distribution as the interface passes over the leading edge and corresponding sharp pulses to lift and moment coefficients amounting to as much as 50% of their steady values. A smaller disturbance occurs when the density interface moves over the trailing edge. Inclination of the interface up to angles of 60 deg to the vertical changes the distribution of the disturbance but makes smaller changes in the magnitudes of the pulses in lift and moment coefficient.

Nomenclature

C_L	=	airfoil lift coefficient
C_{L_0}	=	steady lift coefficient at density ρ_1
C_M	=	airfoil moment coefficient
C_{M_0}	=	steady moment coefficient at density ρ_1
C_p	=	pressure coefficient, $\Delta p/(\rho_1 U^2/2)$
c	=	airfoil chord
F_i	=	Fourier transform of potential
k	=	Fourier transform variable
p	=	perturbation pressure
Q	=	Green's function for supplementary potentials
U	=	undisturbed freestream velocity
v	=	local velocity normal to airfoil
x	=	horizontal coordinate
y	=	vertical coordinate
α	=	airfoil angle of attack
β	=	$(\rho_1 - \rho_2)/(\rho_1 + \rho_2)$
Γ_0	=	circulation of basic vortex
γ	=	vorticity distribution on airfoil
$\gamma(y)$	=	vorticity on density interface
γ_w	=	wake vorticity
γ_0	=	steady-state vorticity distribution on airfoil
$\gamma_0^{(1)}$	=	airfoil shape-related vorticity
$\gamma_0^{(2)}$	=	vorticity to satisfy Kutta condition
Δp	=	local pressure difference across airfoil
Δv	=	velocity difference across interface
η	=	vertical coordinate
η_*	=	vertical coordinate of image vortex
ϑ	=	angle of density interface
λ	=	position of density interface
ξ	=	horizontal coordinate
ξ_*	=	horizontal coordinate of image vortex
ρ_1	=	density upstream of interface
ρ_2	=	density downstream of interface
$\varphi_i^{(j)}$	=	supplmentary potentials
φ_0	=	basic vortex potential

Received 10 December 2003; revision received 21 May 2003; accepted for publication 21 May 2003.

*Richard L. and Dorothy M. Hayman Professor, Emeritus, Mechanical Engineering and Jet Propulsion. Fellow AIAA.

I. Introduction

THE motion of gases with large density nonuniformities assumes importance in situations where combustion, heat transfer, and mixing processes are involved. Incidents that arise in gas turbine aerodynamics range from the ingestion of density stratified airflow into large fans to the strongly nonuniform density field presented to the high-pressure turbine originating from temperature fluctuations introduced by the primary burner. A key feature that differentiates the study of flowfields with nonuniform density is the vorticity generated through the interaction of the density gradients with pressure fields associated with objects about which the flow takes place. For an airfoil passing through a fluid of nonuniform density, the vorticity thus generated induces additional velocities normal to the airfoil and thus affects the vorticity distribution required to satisfy the prescribed airfoil shape. In addition, the spatial variations of density subject the airfoil to an unsteady induction as it passes through them generating a trailing vortex sheet and imposing virtual mass contributions to the loading corresponding to those generated by unsteady motion of the airfoil itself.

The classical theory of airfoils in unsteady motion grew out of the effort to understand wing flutter[1,2] and to understand the response of an airfoil to a gust.[3] The work of von Kármán and Sears[4] presented a unified treatment of thin airfoils in unsteady motion, encompassing both the small-amplitude motion of an airfoil or an airfoil–aileron combination as well as the response to a gust, and established the basis for the subsequent development of the field.

The validity of this two-dimensional, first-order perturbation theory rests on the assumption that both the vortical disturbances transported by the stream and the flowfield disturbances introduced by

the body or by the boundaries confining the flow were small. When this latter condition is violated, difficulties in treating this problem accurately arise from the fact that the behavior of the flowfields of the disturbing obstacles and of the vortical disturbances cannot readily be separated, that is, the distortion of the vorticity is an essential component of the solution, a situation examined by Lighthill[5] in his detailed analysis of drift. To capture features that escape the first-order theory, Goldstein and Atassi[6] carried out a second-order theory, complete in the sense that magnitudes of the disturbance field and the vorticity field are distinguished and treated according to the methods of matched asymptotic expansions.

When the field consists of regions of differing but constant density, vorticity is generated only at the sharp interfaces, and the bulk of the flow remains irrotational. Then the field consists of regions of potential flow matched across the density interfaces. Moreover, if the disturbances to the flowfield are of perturbation order the shape of the interface is preserved to that order as the flow is convected through the region of interest.

In an extension of thin airfoil theory to include motion in fields of nonuniform gas density, the present author[7] investigated the response of a lifting thin airfoil to its passage through a field containing a strong, plane density interface. The resulting transient forces, moments, and local pressure gradients were large enough to merit consideration in load and stability analysis. In this example the fact that the flow disturbance caused by the airfoil was small allows a degree of linearization but still allows the relative difference of gas densities to be large. Two results of this analysis simplified the work substantially. First, the issue of just how Kelvin's theorem should be extended to accommodate contours that include a density interface was resolved, allowing treatment of the trailing vortex sheet in the familiar manner. Second, it was found that the flow induced by a simple singularity on one side of the density interface was equivalent to placing a corresponding simple singularity of appropriate strength in the image point in the plane interface. This allowed a direct extension of the classical unsteady airfoil theory, for example, von Kármán and Sears,[4] to include this special case of inhomogeneous density fields.

The results of this work encouraged Covert, Tan, and their students in the Gas Turbine Laboratory of Massachusetts Institute of Technology to investigate numerically the corresponding problem for heavily loaded airfoil cascades including significant issues of boundary-layer distortion by the induced pressure gradients and some effects of compressibility. This was reported by Ramer[8] and Wijesinghe,[9] where more complex regions of density nonuniformity were examined, including the technologically important periodic influx of density variation. These studies have been continued by Wijesinghe et al.[10]

One of the classical approaches to the theory of steady motion of a thin airfoil through a uniform fluid, and the one that will be followed here, consists of constructing the distribution of vorticity along the proposed mean line, which ensures that the flow will move tangentially to the mean line. Thus if the desired mean line has the shape $\eta(x)$, where η is the vertical coordinate of the mean line, $-c/2 < x < c/2$, the distribution $\gamma_0(\xi)$ of clockwise vorticity must be such that

$$\frac{1}{2\pi}\int_{-c/2}^{c/2}\frac{\gamma_0(\xi)\,\mathrm{d}\xi}{x-\xi} = -U\,\frac{\mathrm{d}\eta(x)}{\mathrm{d}x} \tag{1}$$

With the mean line shape prescribed, this is an integral equation for $\gamma_0(\xi)$, where it is implied that the integral is taken as its Cauchy principal value. This admits the addition of a homogeneous solution, which in this case is fixed by satisfying the Kutta condition. The most familiar example is the flat-plate airfoil at angle of attack α, $\mathrm{d}\eta/\mathrm{d}x = -\alpha$, for which the vorticity distribution

$$\gamma_0^{(1)} = -2U\alpha\left[\xi\Big/\sqrt{(c/2)^2-\xi^2}\right] \tag{2}$$

satisfies the integral equation, but the solution

$$\gamma_0^{(2)} = 2U\alpha\frac{c/2}{\sqrt{(c/2)^2-\xi^2}} \tag{3}$$

of the homogeneous equation must be added to ensure regularity at the trailing edge. Their sum

$$\gamma_0(\xi) = \gamma_0^{(1)} + \gamma_0^{(2)} = 2U\alpha\sqrt{(c/2-\xi)/(c/2+\xi)} \tag{4}$$

then gives the familiar vorticity distribution for a lifting flat plate.

When the airfoil passes through a fluid of nonuniform density, vorticity is generated within the region of nonuniform density by the pressure field imposed by the airfoil. The vorticity thus generated induces additional velocities normal to the airfoil and thus affects the vorticity distribution required to satisfy the prescribed airfoil shape. Consequently the integral equation corresponding to Eq. (1) has additional terms describing this induction and additional contributions to the solution required to satisfy the Kutta condition. In the present case the density gradient and the generated vorticity are confined to the plane interface, and, as will be seen in the following analysis, this offers a clear simplification.

II. Point Vortex Moving near a Plane Density Interface

Consider a density interface that divides the plane along the vertical axis with fluid of density ρ_1 in the right half-plane and fluid of density ρ_2 in the left (Fig. 1). A clockwise vortex of perturbation circulation γ_0 is located at the point ξ, η moving with velocity components $\dot{\xi}$, $\dot{\eta}$. The potential of this vortex is

$$\varphi_0(x, y; t) = -(\Gamma_0/2\pi)\tan^{-1}[(y-\eta)/(x-\xi)] \tag{5}$$

and if the density were uniform this would constitute the complete representation in the entire plane. The presence of the density jump alters the solution in both half-planes. These supplementary solutions we call φ_1 and φ_2 for the right and left half-planes, respectively. Because the basic singularity, Eq. (1), is the only actual singularity in the problem, the supplementary potential φ_1 must be regular in the right half-plane, and the supplementary potential φ_2 must be regular in the left half-plane. Thus, the solutions will consist of $\varphi_0 + \varphi_1$ for $x > 0$ and $\varphi_0 + \varphi_2$ for $x < 0$. Aside from being analytic functions with appropriate behavior for large x, y, these supplementary potentials must ensure that the velocity normal to the interface is equal on both sides, namely,

$$\frac{\partial\varphi_1}{\partial x}(0, y) = \frac{\partial\varphi_2}{\partial x}(0, y) \tag{6}$$

when $x = 0$. Furthermore, the perturbation pressure must be continuous across the density jump:

$$\rho_1\frac{\partial(\varphi_0+\varphi_1)}{\partial t}(0, y) = \rho_2\frac{\partial(\varphi_0+\varphi_2)}{\partial t}(0, y) \tag{7}$$

The solution can be carried out by applying Fourier transforms with respect to y in each half-plane and matching them with the transforms of Eqs. (6) and (7). Originally, in Marble[7] the form of the

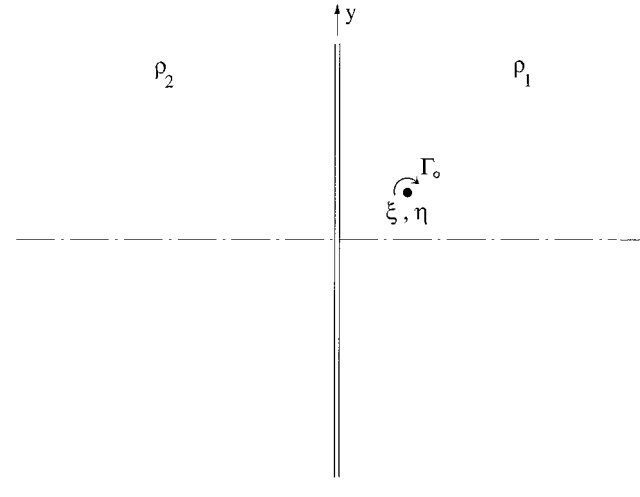

Fig. 1 Basic vortex of circulation Γ_0 moving near a density interface.

result was conjectured and later shown to be correct. Because it will prove useful in subsequent analysis, the Fourier transform solution is given in the Appendix.

Following either path, it transpires that

$$\varphi_1^{(1)} = -\beta(\Gamma_0/2\pi)\tan^{-1}[(y-\eta)/(x+\xi)] \tag{8}$$

$$\varphi_2^{(1)} = -\beta(\Gamma_0/2\pi)\tan^{-1}[(y-\eta)/(x-\xi)] \tag{9}$$

where it is convenient to define

$$\beta = (\rho_1 - \rho_2)/(\rho_1 + \rho_2) \tag{10}$$

The supplementary potential in the right half-plane consists of a vortex of strength $\beta\Gamma_0$ at the image point in the left half-plane, and the supplementary potential for the left half-plane is a vortex of strength $\beta\Gamma_0$ located at the position of the original vortex. This representation of the flow is shown in Figs. 2a and 2b for the right half-plane and the left half-plane respectively when the basic vortex is located in the right half-plane. When the basic vortex is located in the left half-plane, the form of the supplementary potentials is modified as the analysis in the Appendix illustrates. Using the superscript to indicate the location of the basic vortex, these potentials are

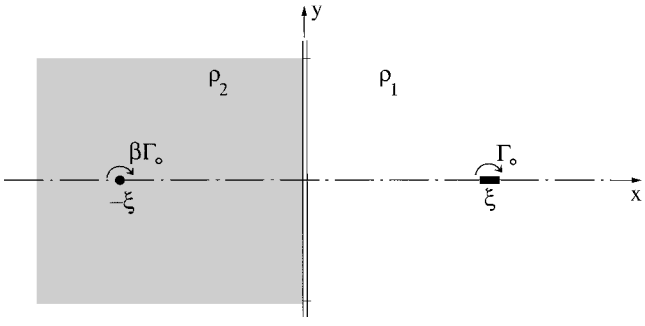

a) $x > 0, \xi > 0$

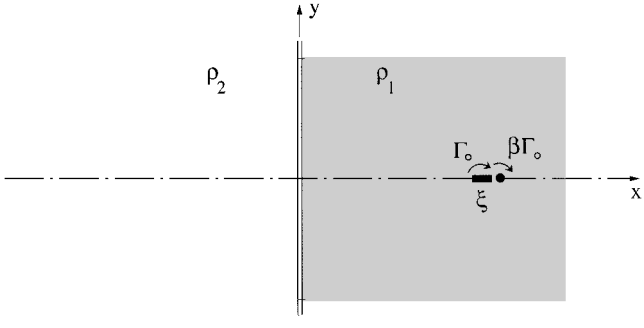

b) $x < 0, \xi > 0$

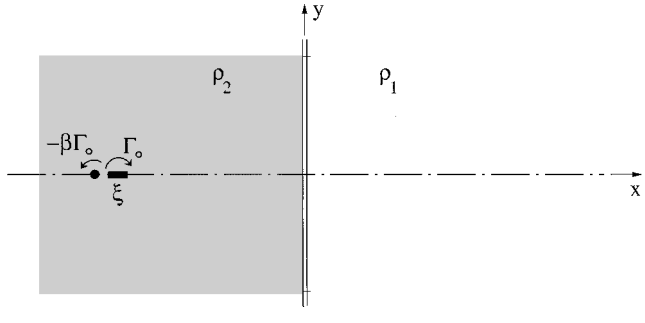

c) $x > 0, \xi < 0$

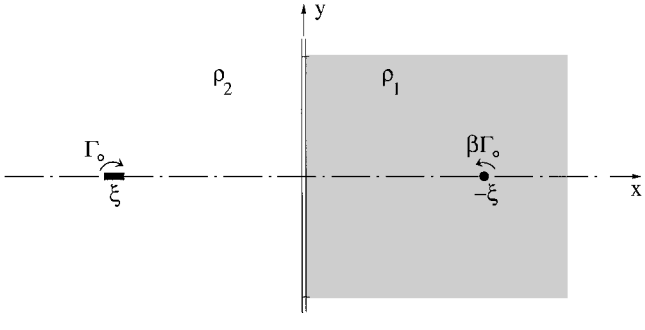

d) $x < 0, \xi < 0$

Fig. 2 Use of image vortices to construct flowfield of a vortex Γ_0 moving near a density interface.

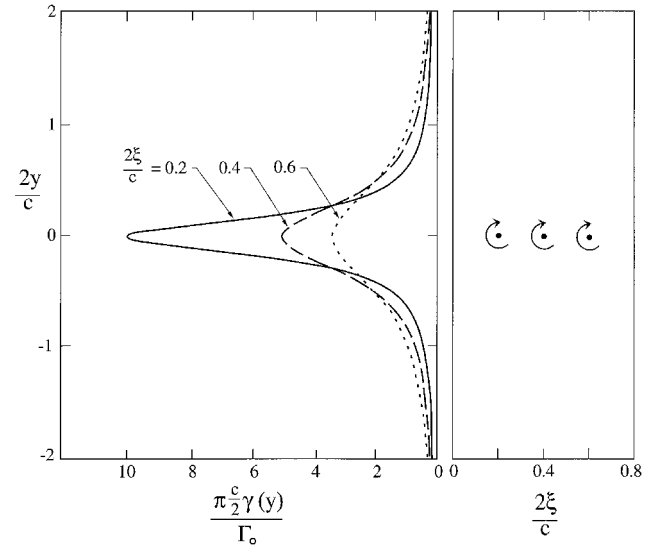

Fig. 3 Vorticity $\gamma(y)$ induced on density interface by basic vortex Γ_0 in various positions.

$$\varphi_1^{(2)} = \beta(\Gamma_0/2\pi)\tan^{-1}[(y-\eta)/(x-\xi)] \tag{11}$$

$$\varphi_2^{(2)} = \beta(\Gamma_0/2\pi)\tan^{-1}[(y-\eta)/(x+\xi)] \tag{12}$$

Recalling that $\xi < 0$, the supplementary potential for the right half-plane, Eq. (11), is a vortex of strength $-\beta\Gamma_0$ at the location of the basic vortex, and the supplementary potential for the left half-plane, Eq. (12), is a vortex of strength $-\beta\Gamma_0$ located at the image point of the basic vortex. This representation is illustrated in Figs. 2c and 2d.

The difference between the supplementary potentials, Eqs. (9) and (10) or Eqs. (11) and (12), represents the vorticity induced at the density interface by the original vortex (Fig. 3). This distribution of vorticity is readily calculated from $\varphi_1^{(1)}$ and $\varphi_2^{(1)}$ and is equal to

$$\gamma(y) = \beta(\Gamma_0/\pi)[\xi/(\xi^2 + y^2)] \tag{13}$$

Clearly the representation of the field by the "image" singularities provides a substantial simplification in the development of the corresponding theory of thin airfoils.

When the density interface is normal to the direction of motion, the induced velocities are normal to the horizontal axis, as can be seen from the image representation. This induced velocity is shown in Fig. 4 for three positions of the basic vortex. The representation of the vertical velocity induced by the interface has four different expressions depending upon the position ξ of the basic vortex and the position x at which the vertical velocity is calculated. These follow directly from the supplementary potentials $\varphi_i^{(j)}$ and can be written

$$v(x;\xi) = \frac{\partial\varphi_i^{(j)}}{\partial y}(x,0;\xi) = \frac{\Gamma}{2\pi}\left\{\frac{(-1)^j\beta}{x+(-1)^{(i+j)}\xi}\right\} \equiv \frac{\Gamma}{2\pi}Q(x;\xi) \tag{14}$$

which defines $Q(x;\xi)$ as a Green's function that gives the vertical velocity induced at the point x by an arbitrary vortex located at point ξ. This notation will prove convenient in formulating the airfoil problem.

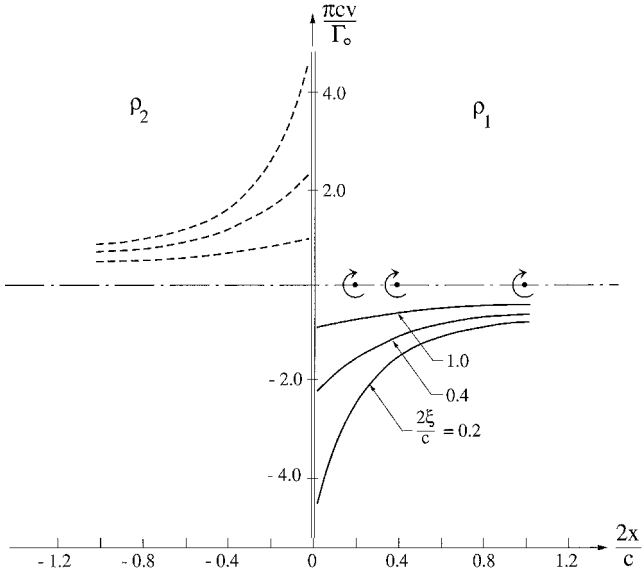

Fig. 4 Vertical velocity v induced by basic vortex Γ_0 in various positions.

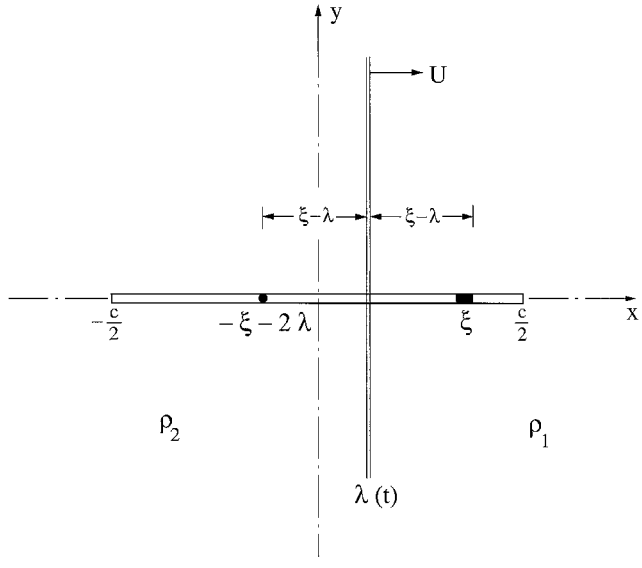

Fig. 5 Configuration for calculaton of velocity induced by a vortex on an airfoil by the image in a convecting density interface at $\lambda(t)$.

III. Vorticity and Load Distributions on Airfoil

Consider a thin airfoil of chord c symmetrically located along the x axis (Fig. 5) in a uniform undisturbed flow with velocity U. For the present we assume the interface to be normal to the flow and, because it is a material interface, it moves over the airfoil with the freestream velocity U. The interaction of a vortex located at ξ, 0 with the interface corresponds to that described in Sec. II because it is only the relative motion that is significant. The distance separating the vortex is no longer ξ but $\xi - \lambda$, where λ is the time-dependent position of the interface. Correspondingly, the image vortex is at the position $-\xi + 2\lambda$. As a consequence, the representations of the supplementary potentials, Eqs. (8) and (12), must be modified as

$$\varphi_1^{(1)} = -\beta\frac{\Gamma_0}{2\pi}\tan^{-1}\left(\frac{y-\eta}{x+\xi-2\lambda}\right) \tag{15}$$

$$\varphi_2^{(2)} = \beta\frac{\Gamma_0}{2\pi}\tan^{-1}\left(\frac{y-\eta}{x+\xi-2\lambda}\right) \tag{16}$$

with corresponding modifications to the Green's function $Q(x, \xi)$.

Because of the presence of the density interface (Fig. 5), the integral relation corresponding to Eq. (1) must be modified to include an additional vorticity $\gamma_1(\xi)$ distributed on the airfoil and by the inclusion of the trailing vortex sheet resulting from the varying circulation caused by the motion of the interface with respect to the airfoil. In detail this relation is

$$-\frac{1}{2\pi}\int_{-c/2}^{c/2}\frac{\gamma_0(\xi)+\gamma_1(\xi)}{x-\xi}\,d\xi + \frac{1}{2\pi}\int_{-c/2}^{c/2}[\gamma_0(\xi)+\gamma_1(\xi)] \times Q(x,\xi)\,d\xi - \frac{1}{2\pi}\int_{c/2}^{\infty}\frac{\gamma_w(\xi_2)}{x-\xi_2}\,d\xi_2 = U\frac{d\eta}{dx} \tag{17}$$

The first integral is the direct induction of vertical velocity caused by the conventional vorticity and the additional vorticity induced on the airfoil. The second integral is the vertical velocity induced by the vorticity distributed on the density interface, expressed using the Green's function $Q(x, \xi)$. The last integral is the vertical velocity induced by the wake vorticity γ_w, generated by the temporal variation of total circulation Γ about the airfoil and shed from the trailing edge $c/2$. Because the wake vorticity element at the location ξ_2 at the time t has been convected with the freestream, it was shed at a time $(\xi_2 - c/2)/U$ earlier. Therefore the change of circulation $d\Gamma\{t - (\xi_2 - c/2)/U\}$ sheds an equal but opposite value $-\gamma_w(\xi_2, t)U\,dt$, which appears at the location ξ_2 at the time t. Because the basic vorticity distribution $\gamma_0(\xi)$ is independent of time, the value of the wake vorticity can be written

$$\gamma_w(\xi_2, t) = -\frac{1}{U}\frac{d}{dt}\int_{-c/2}^{c/2}\gamma_1\left\{\xi, t - \frac{\xi_2 - c/2}{U}\right\}d\xi \tag{18}$$

This argument involves the application of Kelvin's theorem, the validity of which must be justified when the contour contains the density interface. The necessary extension of Kelvin's theorem was detailed in Ref. (7). Because the shed vorticity is convected with the main stream, it does not move with respect to the density interface and consequently, to the order of our calculation, does not interact with it. The right-hand side of Eq. (17) is simply the vertical velocity required by the prescribed shape of the airfoil.

As noted in connection with Eq. (1), the known vorticity $\gamma_0(\xi)$ satisfies the condition on airfoil shape. Moreover, because the Green's function $Q(x; \xi)$ is known, the first term of the second integral is known also, and Eq. (17) can be written more compactly as

$$\int_{-c/2}^{c/2}\frac{\gamma_1(\xi)}{x-\xi}\,d\xi - \int_{-c/2}^{c/2}\gamma_1(\xi)Q(x;\xi)\,d\xi + \int_{c/2}^{\infty}\frac{\gamma_w(\xi_2)}{x-\xi_2}\,d\xi_2 = \int_{-c/2}^{c/2}\gamma_0(\xi)Q(x,\xi)\,d\xi \tag{19}$$

This is then the integral equation for the vorticity distribution $\gamma_1(\xi)$, which can be solved numerically, account being taken to satisfy the Kutta condition as described in the Introduction. When one considers a situation shown in Fig. 5 where the interface is convecting over the airfoil, the location of the interface $\lambda(t)$ moves with the freestream velocity, that is, $d\lambda/dt = U$. Consequently, the solution of Eq. (19) must be carried out for each time value or position of the interface.

With the vorticity distribution on the airfoil known, the pressure difference Δp between the upper and lower surfaces can be calculated from the linearized equation of motion written along the upper surface and the lower surface of the airfoil. Because $u(x, 0+, t) - u(x, 0-, t) \equiv \gamma(x, t)$,

$$\rho\left(\frac{\partial\gamma}{\partial t} + U\frac{\partial\gamma}{\partial x}\right) = -\frac{\partial\Delta p}{\partial x} \tag{20}$$

which can be integrated from the trailing edge, where $\gamma(c/2) = 0$ and $\Delta p(c/2) = 0$. The form of the result depends upon the position λ of the interface and the position x at which the pressure difference is being computed. To illustrate this, consider the configuration of

Fig. 5, where the density interface is passing over the airfoil and calculate the pressure difference at a point x to the left of the interface. Integrating from the point x to the interface,

$$\rho_2 \int_x^{\lambda} \frac{\partial \gamma}{\partial t}\, dx_1 + \rho_2 U[\gamma(\lambda) - \gamma(x)] = -\Delta p(\lambda) + \Delta p(x) \quad (21)$$

In continuing the integration from the interface to the trailing edge, it must be recalled that the velocity normal to the interface and the pressure are continuous across the interface and therefore

$$\rho_1 \int_{\lambda}^{c/2} \frac{\partial \gamma}{\partial t}\, dx_1 + \rho_1 U[\gamma(c/2) - \gamma(\lambda)] = -\Delta p(c/2) + \Delta p(\lambda) \quad (22)$$

Eliminating $\Delta p(\lambda)$ between Eqs. (21) and (22) and taking into account of the vanishing of the vorticity and the pressure difference at the trailing edge, the pressure difference at the point x of the airfoil is

$$\Delta p(x) = -\rho_2 U \gamma(x) - (\rho_1 - \rho_2) U \gamma(\lambda) + \rho_2 \int_x^{\lambda} \frac{\partial \gamma}{\partial t}\, dx_1 + \rho_1 \int_{\lambda}^{c/2} \frac{\partial \gamma}{\partial t}\, dx_1 \quad (23)$$

When the interface is either upstream of the airfoil leading edge or downstream of the trailing edge, the contribution $(\rho_1 - \rho_2)U\gamma(\lambda)$ is absent.

The manner in which the flowfield is affected by inclination of the density interface can be seen by examining the vortex images generated by a vortex element $\Gamma_0(\xi)$ located at a point on the airfoil downstream of the density interface (Fig. 6a). The supplementary flow in the region to the right of the interface is represented by the vortex of strength $\beta\Gamma_0(\xi)$ at the image point ξ_*, η_*. Because this point is out of the plane of the airfoil, it induces both normal and tangential components, of which only the normal component is of interest to us. On the other hand, the supplementary flow in the region to the left of the density interface is represented by a vortex of strength $\beta\Gamma_0(\xi)$ located at the point of the original vortex (Fig. 6b) and thus is independent of the orientation of the density interface. Consequently, the effect of interface inclination on the velocity induced normal to the airfoil is entirely on that portion of the airfoil downstream of the intersection of the interface with the airfoil. The details of that induced velocity will be examined in some detail.

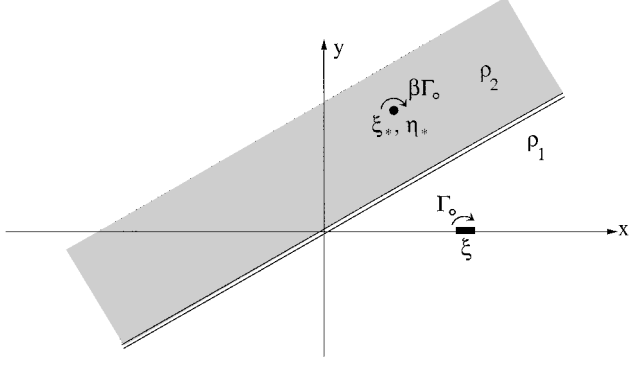

a) $x > 0$

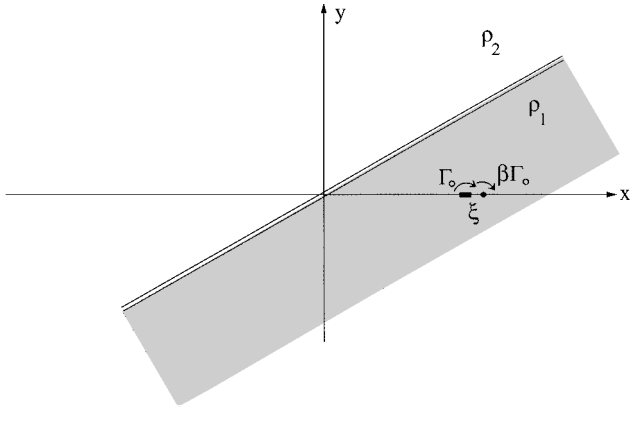

b) $x < 0$

Fig. 6 Location of image vortices for inclined density interface for calculation of induced velocity at point x in plane of airfoil, basic vortex Γ_0 at $\xi > 0$.

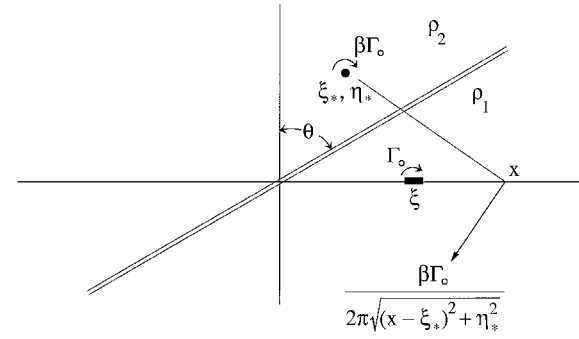

Fig. 7 Velocity induced in airfoil plane by image vortex for an inclined density interface.

Consider the inclined interface shown in Fig. 7 with a vortex element $\Gamma_0(\xi)$ located on the axis in the plane of the airfoil and downstream of the interface inclined at an angle ϑ with respect to the vertical axis. The image vortex is located at $\xi_* = -\xi \cos 2\vartheta$, $\eta_* = \xi \sin 2\vartheta$, and induces a vertical velocity component

$$v(x, 0) = -\frac{\beta\Gamma_0}{2\pi} \frac{x - \xi_*}{(x - \xi_*)^2 + (\eta_*)^2} \quad (24)$$

in the plane of the airfoil. This can be more conveniently rewritten in a dimensionless form

$$\frac{2\pi v\xi}{\beta\Gamma_0} = -\frac{x/\xi + \cos 2\vartheta}{(x/\xi)^2 + 2(x/\xi)\cos 2\vartheta + 1} \quad (25)$$

and from Eq. (25) it is clear that the vertical velocity induced vanishes at some point to the right of the interface when $\vartheta > \pi/4$. The vanishing of the numerator of Eq. (25) is seen from Fig. 7 to occur when the point x at which the induced velocity is calculated lies directly below the position of the image vortex, and consequently the entire induced velocity is parallel to the airfoil surface. To show the situation in more detail, the distribution of induced vertical velocity in the plane of the airfoil is shown in Fig. 8a for an interface inclination of 60 deg. For this orientation of the interface, the numerator vanishes for $x/\xi = 0.5$. For large values of x/ξ, the vertical velocity behaves as $(x/\xi)^{-1}$ so that a maximum downwash occurs at some value of $x/\xi > 0.5$. From Eq. (25) this value is $x/\xi = -\cos 2\vartheta + \sin 2\vartheta$, and this maximum downwash velocity is

$$2\pi v\xi/\beta\Gamma_0 = -1/2 \sin 2\vartheta \quad (26)$$

To the left of the interface, that is, upstream, the induction is independent of interface orientation and consequently identical with that shown in Fig. 4.

When the inclination of the interface is at 30 deg, the vanishing of the induced velocity and the maximum downwash do not occur within the region of validity, that is, for $x/\xi > 0$. This situation is shown in Fig. 8b as well as the downwash distribution upstream of the interface.

Two additional features of this flowfield should be mentioned. First, the induction pattern is altered when the position of the basic vortex $\Gamma_0(\xi)$ is to the left of the interface, that is, for example, $\xi < 0$ in Fig. 7. Then the downwash in the plane of the airfoil is affected by the inclination of the interface for positions ahead of

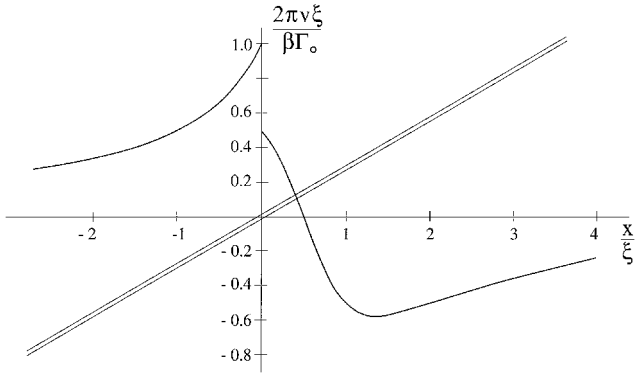

a) ϑ = 60 deg

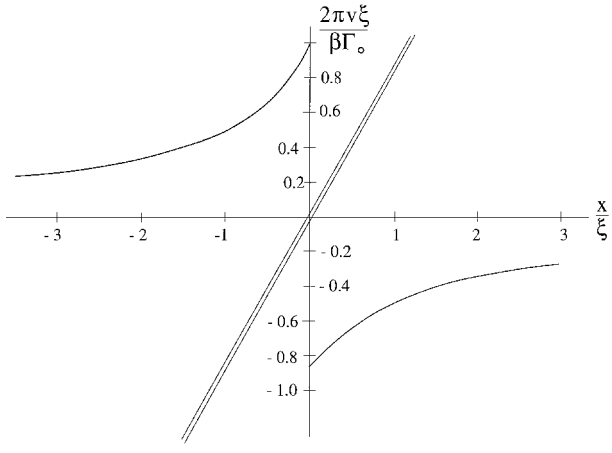

b) ϑ = 30 deg

Fig. 8 Velocity v normal to airfoil induced by interaction of vortex Γ_0 with interface inclined at an angle ϑ.

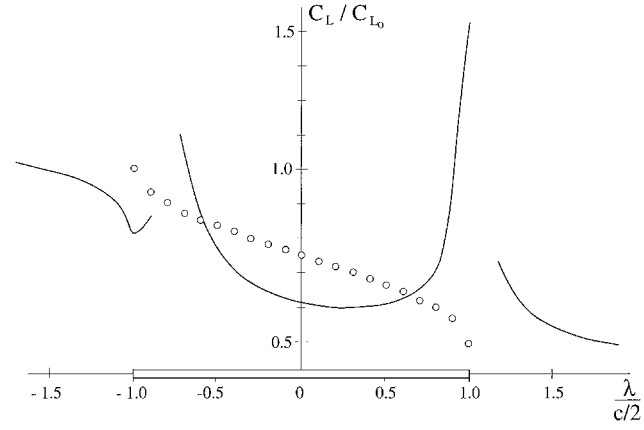

a) C_L/C_{L_0}

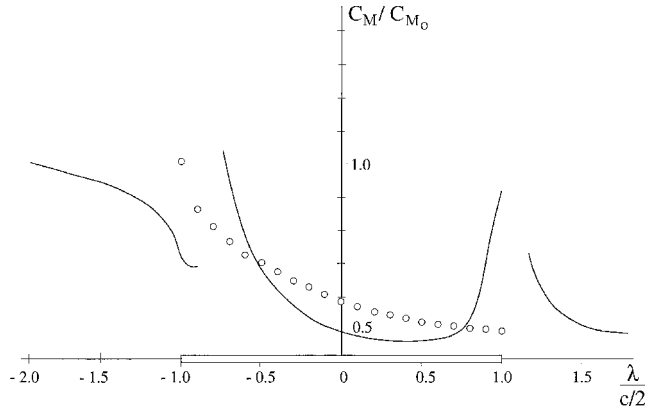

b) C_M/C_{M_0}

Fig. 9 Lift and moment coefficients induced on flat-plate airfoil by passage of density interface: ρ_2/ρ_1 = 0.5 and ϑ = 0 deg.

the interface, $x < 0$, and unaffected at positions downstream of the interface, $x > 0$. The second point of interest is that the induced downwash distribution is unchanged by a change of sign of the inclination angle from ϑ to $-\vartheta$. This can be formally deduced from Eq. (25) or inferred from Fig. 7.

IV. Application to Flat Plate Airfoil

The results obtained in Secs. II and III can be applied to any lifting thin airfoil for which the solution in steady homogenious flow is known. Specifically, the steady-state vorticity $\gamma_0(\xi)$ is required. For the behavior of the flat-plate airfoil, which shall be examined in the present section, the steady vorticity distribution in a flow of uniform density is

$$\gamma_0(\xi) = 2U\alpha\sqrt{(c/2-\xi)/(c/2+\xi)} \tag{27}$$

Numerical calculations for the response of the airfoil to the passage of a density interface are carried out for a density ratio of $\rho_2/\rho_1 = 0.5$, making $\beta = \frac{1}{3}$, and an angle of attack α of 0.1 radian. The pressure coefficient distribution, $C_p(x) = \Delta p(x)/(\rho_1 U^2/2)$, follows from Eq. (23) after the supplementary vorticity $\gamma_1(\xi)$ has been determined from Eq. (19) for the desired time sequence [positions $\lambda(t)$ of the interface]. From the pressure coefficient, the lift coefficient and moment coefficient follow by appropriate integration over the airfoil chord. In carrying out the calculations the airfoil chord was divided into elements, a point vortex was located at the quarter point of each element, and the downwash was computed at the three-quarter point of each element. The resulting matrix was inverted to find values of $\gamma_1(\xi)$ at the discrete points of the airfoil. For most of the calculations, 20 elements were used. The results were checked by selected cases using 40 elements.

Figures 9a and 9b show respectively the lift coefficient and moment coefficient as a normal interface, $\vartheta = 0$, approaches and passes over the airfoil. In each case the coefficients are normalized by their steady values at the initial density ρ_1.

Consider first the response of the airfoil lift coefficient to the passage of a normal interface (Fig. 9a). As the interface approaches the airfoil, the downwash induced by the density interface begins to reduce the lift coefficient about a half-chord length upstream of the leading edge. A sharp pulse of at least 25% follows as the interface passes over first quarter-chord and a nearly continuous reduction to the final value of 0.5 as it passes downstream. The origins of this response are apparent from the vorticity and pressure distributions (Figs. 10a and 11a) when the density interface is upstream of the leading edge, $2\lambda/c = -1.2$. The strong downwash and consequent increased pressure on the upper surface results from the image of the large values of γ_0 near the leading edge of the airfoil. Note the singularity as ξ approaches $-c/2$ in Eq. (27). With the interface to the left of the leading edge, the image vortex creates a downwash on the airfoil, similar to the configuration shown in Fig. 2a. As the interface passes downstream of the leading edge (Figs. 12a and 13a), the large values of γ_0 lie to the left of the interface, and, as indicated in Figs. 2b, the image vortex induces a strong upwash producing a sharp pressure reduction on the upper surface of the airfoil.

It is interesting to contrast this result with that of the the classical sharp-edge gust.[4] The gust has no influence when it is upstream of the leading edge, formally because the vorticity is distributed uniformly and has no range of influence. On the other hand, the trailing vortex sheet of the gust problem continues to influence the airfoil behavior when it has moved more than five chord lengths downstream, whereas that of the density interface is quite short. The difference lies in the fact that the vorticity distribution on the airfoil passing through a density interface is identical when the interface is far upstream or far downstream. As a consequence, the wake

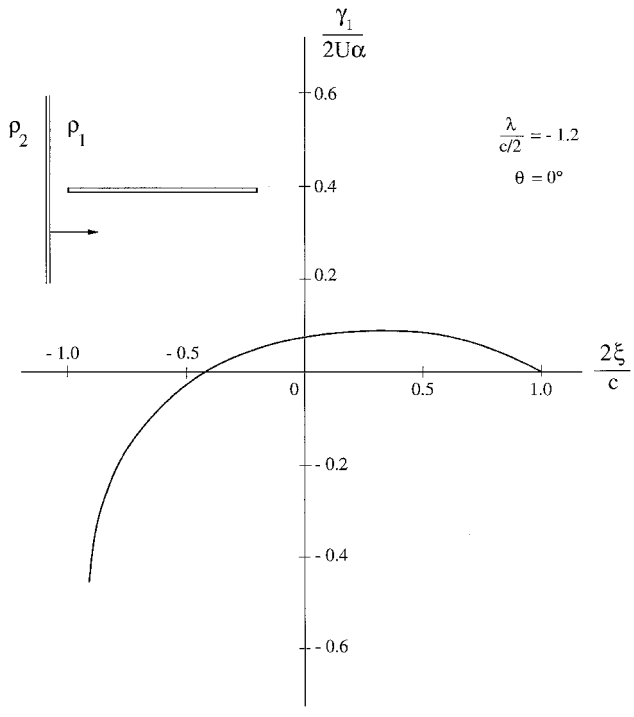

a) $\lambda/(c/2) = -1.2$

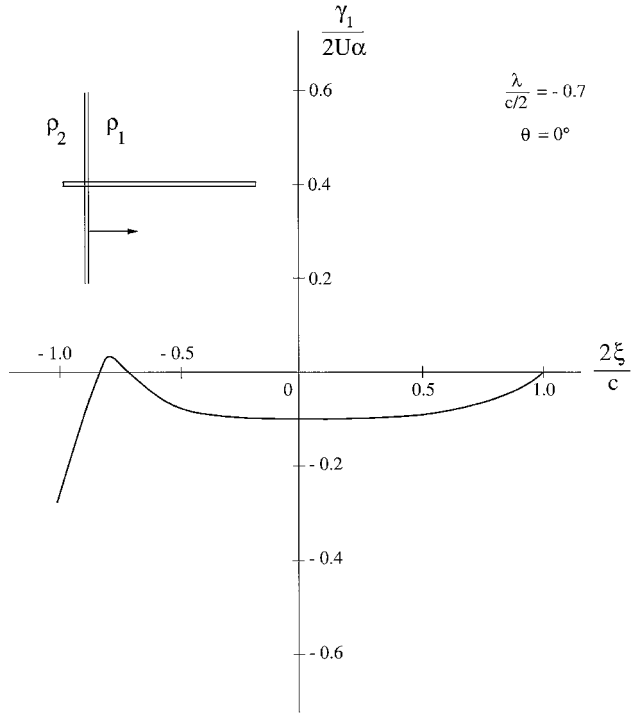

b) $\lambda/(c/2) = -0.7$

Fig. 10 Vorticity distribution induced on flat-plate airfoil by interface normal to flow: $\rho_2/\rho_1 = 0.5$.

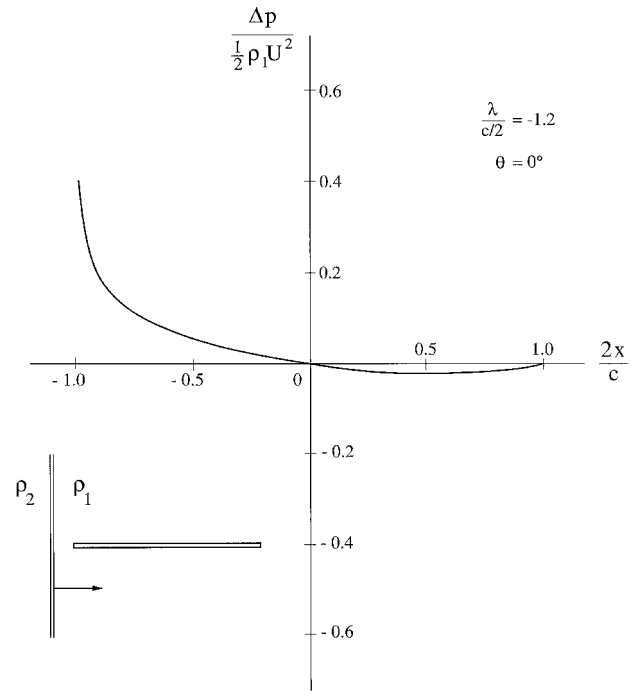

a) $\lambda/(c/2) = -1.2$

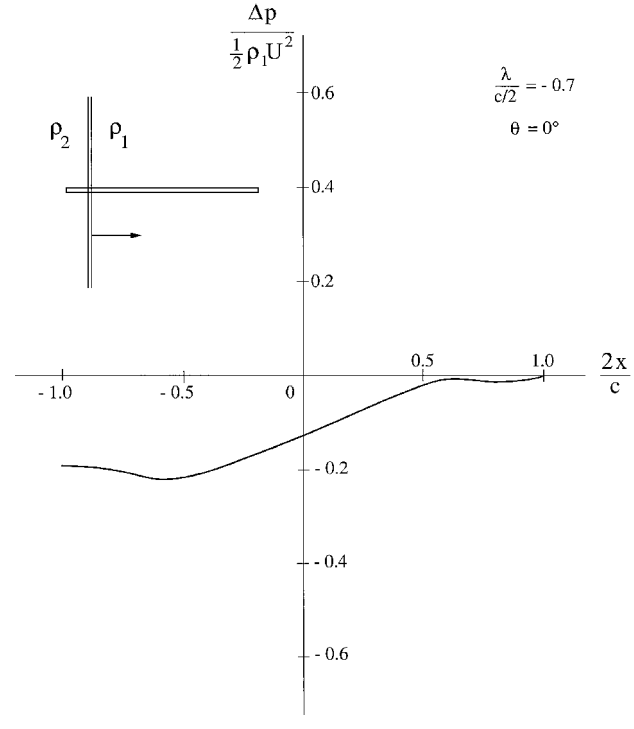

b) $\lambda/(c/2) = -0.7$

Fig. 11 Pressure distribution induced on flat-plate airfoil by interface normal to flow: $\rho_2/\rho_1 = 0.5$.

contains no net vorticity, behaves like a vortex pair, and its influence attenuates like $1/\lambda^2$.

The corresponding moment coefficient ratio (Fig. 9b) shows the strong counterclockwise moment caused by unloading the leading-edge region as the density interface approaches the airfoil. This is followed by a strong clockwise moment as the leading edge is impulsively loaded when the interface passes the leading edge. These moment variations correspond to the loading pulses shown in Fig. 9a. The load and moment changes as the interface passes the trailing edge result from the strong response of the Kutta condition to the change of sign on the induction as the interface passes the trailing edge.

The pressure distribution (Fig. 11a), the lift coefficient (Fig. 9a), and the moment coefficient (Fig. 9b) follow from the pressure difference relation [Eq. (23)]. The vorticity distribution $\gamma(x)$ is the sum of the steady-state distribution γ_0 and that induced by density interface and the wake γ_1. Because it is independent of time, γ_0 does not contribute to the virtual mass integrals. The remaining two terms represent the interaction of the vorticity $\gamma_0 + \gamma_1$ with the freestream flow of the density in which the vorticity is located at that moment. Therefore if the vorticiy γ_1 is suppressed, the remaining terms of

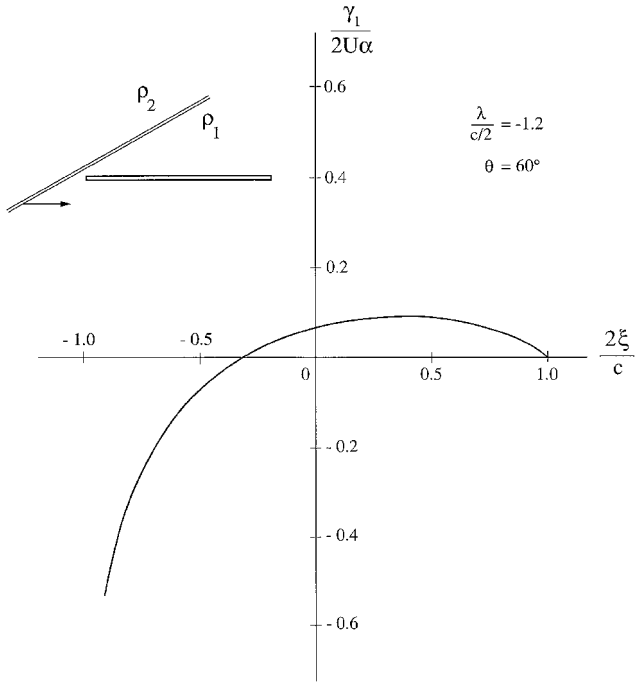

a) $\lambda/(c/2) = -1.2$

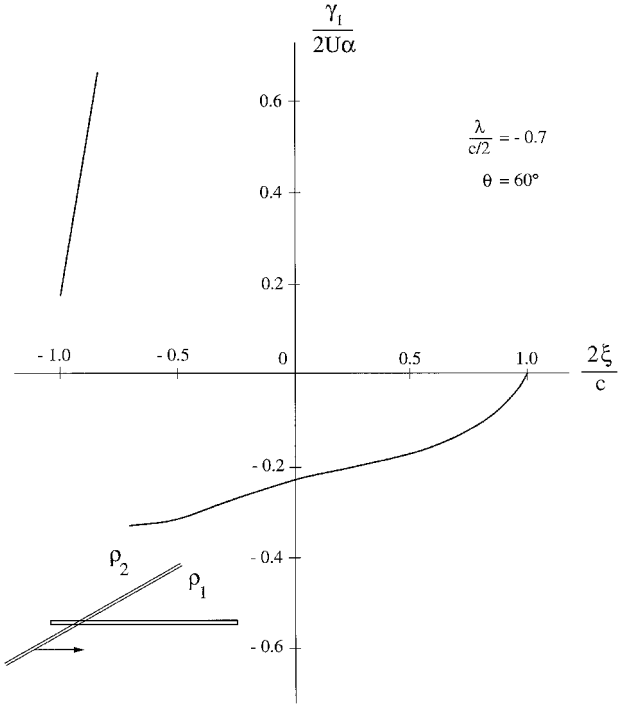

b) $\lambda/(c/2) = -0.7$

Fig. 12 Vorticiy distribution induced on flat-plate airfoil inclined at 60 deg to normal: $\rho_2/\rho_1 = 0.5$.

Eq. (23) give

$$\Delta p(x) = -\rho_2 U \gamma_0(x) - (\rho_1 - \rho_2) U \gamma_0(\lambda) \tag{28}$$

If the lift and moment coefficients are now calculated using the loading given by Eq. (28), the differences from those calculated from the full equation (23) represent the contributions of the interface vorticity, the trailing vortex sheet, and the virtual mass.

For the flat-plate airfoil whose basic vorticity distribution is given by Eq. (27), the loading given by Eq. (28) can be integrated to give expressions for the corresponding lift and moment coefficients as

$$C_L/C_{L0} = 1 - (1 - \rho_2/\rho_1)[1 - (1/\pi)\cos^{-1}\lambda] \tag{29}$$

$$C_M/C_{M0} = 1 - (1 - \rho_2/\rho_1) \times \left[1 - (1/\pi)\cos^{-1}\lambda + (\lambda/\pi)\sqrt{1 - \lambda^2}\right] \tag{30}$$

These values are shown as circles on the lift coefficient and moment coefficient plots (Figs. 9a and 9b). The differences from the actual values show the magnitude and location of the contributions of the density interface vorticity. As might be anticipated, the differences

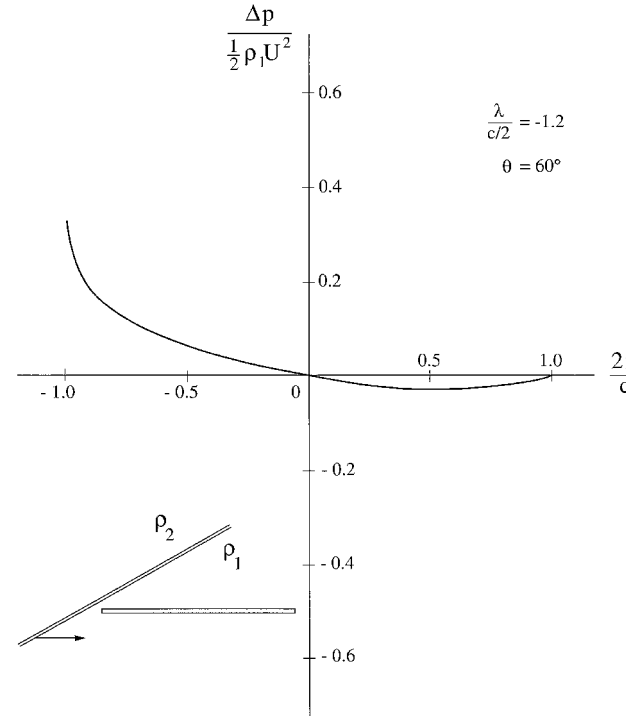

a) $\lambda/(c/2) = -1.2$

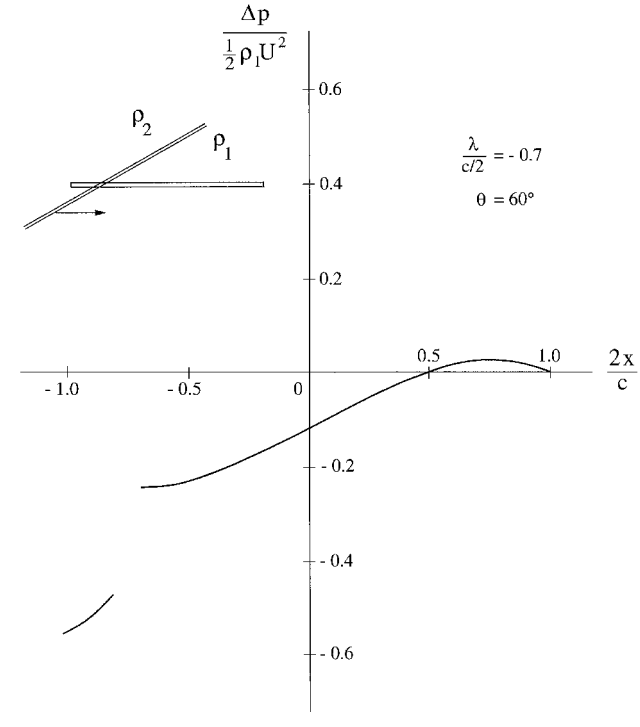

b) $\lambda/(c/2) = -0.7$

Fig. 13 Pressure distribution induced on flat-plate airfoil inclined at 60 deg to normal: $\rho_2/\rho_1 = 0.5$.

are largest during the entry of the leading edge into the new density field.

When the density interface is inclined with respect to the the plane of the airfoil, changes in the lift and moment responses result from the alterations in the positions of the vortex images that were discussed and illustrated in Figs. 6–8. Consider first the induced vertical velocity when interface is inclined at 60 deg shown in Fig. 8a. In this case the image vortex lies to the right of the intersection of the interface with the airfoil plane and consequently influences the induction on the airfoil when this intersection is upstream of the leading edge. The resulting lift and moment coefficients Figs. 14a and 14b show the earlier arrival of the image vortex, but this effect is somewhat counteracted by the fact that a smaller component of the induced velocity is directed normal to the airfoil as indicated in Fig. 7. That this influence continues as long as the large values of γ_0 are in range of the interface is more apparent from comparison of the vorticity distributions (Fig. 12) and pressure distributions (Fig. 13) with those for the normal interface (Figs. 10 and 11). Changes of comparable magnitude in the lift and moment coefficient are evident (Fig. 14), as the interface passes over the trailing edge.

When the interface is inclined at an angle of 30 deg, the image vortex for the region $x > 0$ lies to the left of the intersection, and the resulting velocity induced normal to the plane of the airfoil is as shown in Fig. 8b. The lift and moment coefficients for this configuration are shown in Figs. 15a and 15b, respectively. As one might anticipate, the results are more similar to those for the normal interface than those for the interface with a 60-deg inclination, particularly in the region near the trailing edge. On the other hand, the

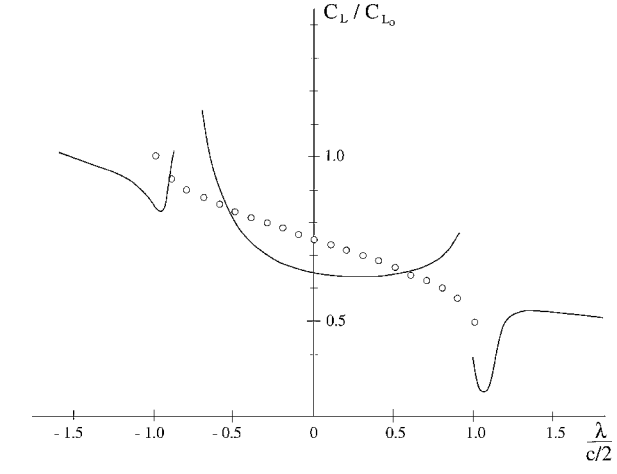

a) C_L/C_{L_0}

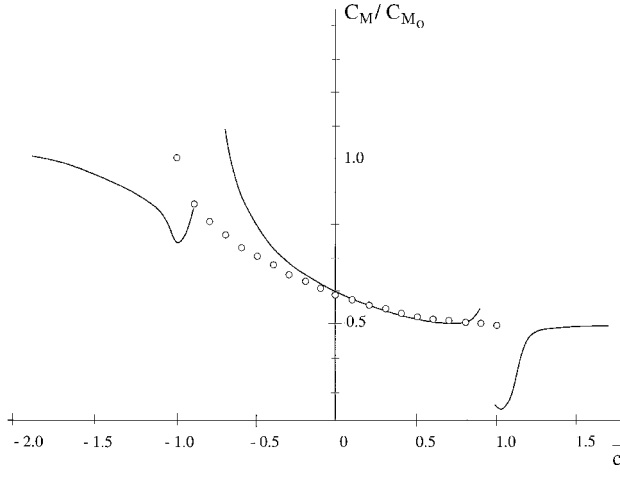

b) C_M/C_{M_0}

Fig. 14 Lift and moment coefficients induced on flat-plate airfoil by passage of density interface: $\rho_2/\rho_1 = 0.5$ and $\vartheta = 60$ deg.

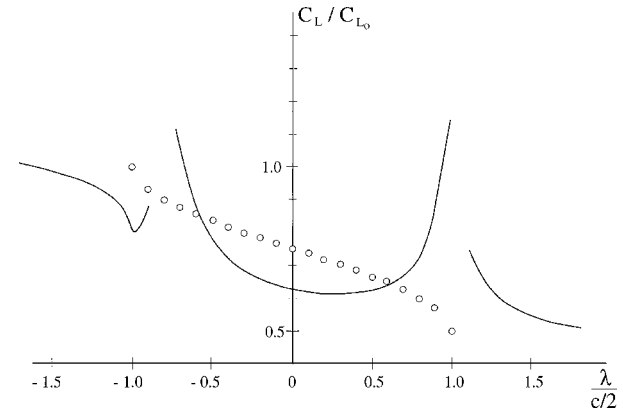

a) C_L/C_{L_0}

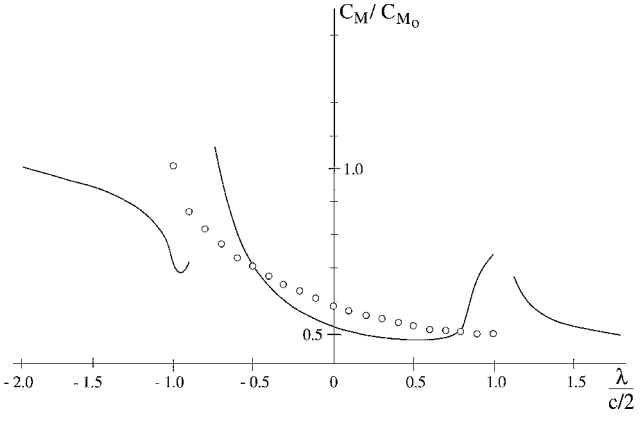

b) C_M/C_{M_0}

Fig. 15 Lift and moment coefficients induced on flat-plate airfoil by passage of density interface: $\rho_2/\rho_1 = 0.5$ and $\vartheta = 30$ deg.

results for the normal interface (Fig. 9) and those for the inclined interface (Figs. 14 and 15) bear more similarity than might be expected, particularly in view of the contrasting vorticity distributions shown in Figs. 10 and 12. It transpires that the large excursions of $\gamma_1(\xi)$ as the interface moves along the airfoil induce large values of $\partial\gamma_1/\partial t$ and correspondingly large contributions from the virtual mass integrals, for example, Eq. (23), and these tend to compensate each other.

In summary, for both the normal and inclined density interface the lift and moment disturbances consist of two distinct parts. The first is the reduction in magnitude of lift and moment associated with the interaction of the steady-state vorticity with the changed density field. This contribution is shown by the circles in Figs. 9, 14, and 15. For the present results, with a density ratio $\rho_2/\rho_1 = 0.5$, this represents a factor of 2 change in these coefficients over a timescale of c/U. The second part is that caused by the induction by the density interface and the associated wake. It consists of pulses at the leading and trailing edges, which, for the load distribution of the present example, have timescales of the order of the time for the density interface to pass overa quarter-chord of the airfoil, that is, $c/4U$. Between these pulses the interface induction can influence values of the coefficients by as much as 20%. These detailed results will differ for airfoil shapes with different chordwise loadings.

Appendix: Solution for Supplementary Potentials

The Fourier transforms of the supplementary potentials φ_i are written

$$F_i(x,k) = \frac{1}{\sqrt{2\pi}} \int_{-\infty}^{\infty} e^{-iky} \varphi_i(x,y)\, dy \qquad \text{(A1)}$$

and its inverse

$$\varphi_i(x, y) = \frac{1}{\sqrt{2\pi}} \int_{-\infty}^{\infty} e^{iky} F_i(x, y)\, \mathrm{d}k \tag{A2}$$

where $i = 1, 2$. Because the φ_i are harmonic functions, the transforms of F_i can be written

$$F_1 = A_1(k) e^{-|k|x} \tag{A3}$$

$$F_2 = A_2(k) e^{|k|x} \tag{A4}$$

Also they must satisfy the transforms of Eqs. (6) and (7)

$$-|k| A_1 e^{-|k|x} = |k| A_2 e^{|k|x} \tag{A5}$$

$$\rho_1 \frac{\partial A_1}{\partial t} e^{-|k|x} - \rho_2 \frac{\partial A_2}{\partial t} e^{|k|x} = -(\rho_1 - \rho_2) \frac{\partial F_0}{\partial t} \tag{A6}$$

where F_0 is the transform of the basic vortex potential, Eq. (5). Because these conditions apply at $x = 0$, they reduce to

$$A_2 = -A_1 \tag{A7}$$

$$\frac{\partial A_1}{\partial t} = -\beta \frac{\partial F_0}{\partial t}(0, k) \tag{A8}$$

When $\xi > 0$, the expression for F_0 is

$$F_0 = -\left(i\Gamma_0 \Big/ \sqrt{2\pi}\right)(1/2k) e^{-k(\xi - x + i\eta)} \tag{A9}$$

when $k > 0$, and

$$F_0 = -\left(i\Gamma_0 \Big/ \sqrt{2\pi}\right)(1/2k) e^{k(\xi - x - i\eta)} \tag{A10}$$

when $k < 0$. Entering these into Eq. (A8) yields

$$\frac{\partial A_1}{\partial t} = -\beta \frac{i\Gamma_0}{\sqrt{2\pi}} \frac{1}{2} \frac{\mathrm{d}\xi}{\mathrm{d}t} e^{-k(\xi + i\eta)} \tag{A11}$$

for $k > 0$ and

$$\frac{\partial A_1}{\partial t} = \beta \frac{i\Gamma_0}{\sqrt{2\pi}} \frac{1}{2} \frac{\mathrm{d}\xi}{\mathrm{d}t} e^{k(\xi - i\eta)} \tag{A12}$$

for $k < 0$, which, using Eq. (A3), can be inverted to give $\partial\varphi_1/\partial t$. This result can, in turn, be integrated with respect to time and finally

$$\varphi_1 = -(\beta\Gamma_0/2\pi) \tan^{-1}[(y - \eta)/(x + \xi)] \tag{A13}$$

valid for $\xi > 0$. In a similar manner the relationship Eq. (A7) and the expression for F_2, Eq. (A4), can be inverted to give

$$\varphi_2 = -(\beta\Gamma_0/2\pi) \tan^{-1}[(y - \eta)/(x - \xi)] \tag{A14}$$

also valid for $\xi > 0$.

The results Eqs. (A13) and (A14) correspond to Eqs. (8) and (9) in the main text. The expressions for the supplementary potentials valid for $\xi < 0$, appearing as Eqs. (11) and (12) in the main text, are obtained by choosing the expressions for F_0, Eqs. (A9) and (A10) that are valid for $\xi < 0$, and following the same procedure.

References

[1]Glauert, H., "The Force and Moment on an Oscillatng Airfoil," British Aeronautical Research Council, R.&M. 1242, London, 1929.

[2]Theodorsen, T., "General Theory of Aerodynamic Instability and the Mechanism of Flutter," NACA TR 496, May 1934.

[3]Kussner, H. G., "Zusammenfassender Bericht uber den instationaren Auftrieb von Flugeln," *Luftfahrtforschung*, Bd. 13, 1936, pp. 410–424.

[4]von Kármán, T., and Sears, W. R., "Airfoil Theory for Non-Uniform Motion," *Journal of the Aeronautical Sciences*, Vol. 5, 1938, pp. 379–390.

[5]Lighthill, M. J., "Drift," *Journal of Fluid Mechanics*, Vol. 1, Pt. 1, 1956, pp. 31–53.

[6]Goldstein, M. E., and Atassi, H. M., "A Complete Second Order Theory for the Unsteady Flow About an Airfoil Due to a Periodic Gust," *Journal of Fluid Mechanics*, Vol. 74, Pt. 4, 1976, pp. 741–765.

[7]Marble, F. E., "Response of a Thin Airfoil Encountering a Strong Density Discontinuity," *Symposium on Aerodynamics and Aeroacoustics*, edited by K.-Y. Fung, World Scientific, Singapore, 1993, pp. 231–255; also *Journal of Fluids Engineering*, Vol. 115, 1993, pp. 580–589.

[8]Ramer, B. E., "Aerodynamic Response of Turbomachinery Blade Rows to Convecting Density Distortions," M.S. Thesis, Dept. of Aeronautics and Astronautics, Massachusetts Inst. of Technology, Cambridge, MA, Jan. 1997.

[9]Wijesinghe, H. S., "Aerodynamic Response of Turbomachinery Blade Rows to Convecting Density Wakes," M.S. Thesis, Dept. of Aeronautics and Astronautics, Massachusetts Inst. of Technology, Cambridge, MA, Sept. 1998.

[10]Wijesinghe, H. S., Tan, C. S., and Covert, E. E., "Aerodynamic Response of Turbomachinery Blade Rows to Convecting Density Wakes," *Journal of Turbomachinery*, Vol. 124, No. 2, 2002, pp. 269–274.

G. M. Faeth
Former Editor-in-Chief